

# A composite likelihood approach to computer model calibration using high-dimensional spatial data

Won Chang, Murali Haran, Roman Olson, and Klaus Keller

November 28, 2021

## Abstract

Computer models are used to model complex processes in various disciplines. Often, a key source of uncertainty in the behavior of complex computer models is uncertainty due to unknown model input parameters. Statistical computer model calibration is the process of inferring model parameter values, along with associated uncertainties, from observations of the physical process and from model outputs at various parameter settings. Observations and model outputs are often in the form of high-dimensional spatial fields, especially in the environmental sciences. Sound statistical inference may be computationally challenging in such situations. Here we introduce a composite likelihood-based approach to perform computer model calibration with high-dimensional spatial data. While composite likelihood has been studied extensively in the context of spatial statistics, computer model calibration using composite likelihood poses several new challenges. We propose a computationally efficient approach for Bayesian computer model calibration using composite likelihood. We also develop a methodology based on asymptotic theory for adjusting the composite likelihood posterior distribution so that it accurately represents posterior uncertainties. We study the application of our new approach in the context of calibration for a climate model.

## 1 Introduction

Complex computer models are often used to approximate real-world processes. These models enable us to conduct virtual experiments that are useful for studying and un-

derstanding complex physical phenomena. A central source of uncertainty regarding computer models, and hence the behavior of the process they are approximating, stems from uncertainty about the value of model input parameters. It is, however, often possible to learn about model parameter values from observations of the system being modeled. Computer model calibration, the methods used to learn about these parameters, involves finding model parameter settings that produce computer model outputs that are most compatible with the observed realization of the process. Statistical computer model calibration is a formal approach to parameter inference based on observations and on computer model output at various parameter settings. A sound approach to computer model calibration accounts for various sources of uncertainties such as measurement error and model structural errors, and results in a probability distribution that summarizes our knowledge about the parameters. Quantifying uncertainties about the parameters carefully is important as this allows for a rigorous quantification of uncertainties about projections based on the model. Here we consider computer model calibration for problems where the observations and the model output are in the form of spatial data.

Computer model calibration can pose nontrivial inferential challenges. In many applications computer model runs are computationally expensive. In this case, model runs are often available at only a limited number of parameter settings. A popular method to overcome this hurdle is the Gaussian process approach (cf. Sacks et al., 1989; Kennedy and O’Hagan, 2001). This method enables calibration with a limited number of model runs using probabilistic interpolation between the model runs. However, this approach faces computational challenges when applied to computer model output that are in the form of high-dimensional spatial data, which are increasingly common in modern science and engineering applications (see e.g. Higdon et al., 2009; Bhat et al., 2010, 2012; Chang et al., 2013).

Some approaches have been developed recently to resolve these computational issues (e.g. Bayarri et al., 2007; Higdon et al., 2008; Bhat et al., 2012; Chang et al., 2013). In this manuscript we propose a new Bayesian approach for calibration with high-dimensional spatial data using composite likelihood methods.

The basic idea of composite likelihood (Besag, 1975, 1977; Lindsay, 1988) is to approximate the original likelihood as a product of computationally cheaper likelihoods. This approach can be easily adapted for spatial modeling in various ways such as conditional likelihood (Vecchia, 1988; Stein et al., 2004), pairwise likelihood (Heagerty and Lele, 1998; Curriero and Lele, 1999; Cooley et al., 2011), and block likelihood (Caragea and Smith, 2006; Eidsvik et al., 2013). Here we construct a calibration method based on block composite likelihood. In particular, we adopt the idea of hybrid composite likelihood proposed by Caragea and Smith (2006) that relies on two components: (i) dependence between block means and (ii) dependence within each block conditioning on its block mean. This composite likelihood approach allows for a substantial reduction in the computational burden for maximum likelihood inference with high-dimensional spatial data. Also, this opens up possibilities for flexible spatial covariance structure that vary depending on each block. Moreover, since the composite likelihood from the block composite likelihood framework is a valid probability model, no further justification is necessary for its use in Bayesian inference.

The remainder of this paper is organized as follows. In Section 2 we outline the basic model calibration framework using Gaussian random fields. In Section 3 we formulate the Bayesian calibration model using block composite likelihood, discuss relevant asymptotic theory and explain how Godambe information may be used to adjust posterior uncertainty when using composite likelihood. In Section 4 we describe an application of our method to a climate model calibration problem using 2-dimensional spatial patterns of ocean temperature change and a relevant simulated example. Finally, in Section 5, we conclude with a discussion and future directions for research.

## 2 Calibration using Gaussian Processes

Here we introduce our computer model calibration framework which consists of two stages: model emulation and parameter calibration (Bayarri et al., 2007; Bhat et al., 2012; Chang et al., 2013). We first construct an ‘emulator’, which is a statistical model interpolating

the computer model outputs as well as providing interpolation uncertainties (Sacks et al., 1989). Using the emulator, we find the posterior density of computer model parameters while taking into account important sources of uncertainty including interpolation uncertainty, model-observation discrepancy, and observational error (Kennedy and O’Hagan, 2001).

We will use the following notation henceforth.  $Y(\mathbf{s}, \boldsymbol{\theta})$  is the computer model output at the spatial location  $\mathbf{s} \in \mathcal{S}$  and the parameter setting  $\boldsymbol{\theta} \in \boldsymbol{\Theta}$ .  $\mathcal{S}$  is the spatial field that we are interested in, usually a subset of  $\mathbb{R}^2$  or  $\mathbb{R}^3$ .  $\boldsymbol{\Theta} \subset \mathbb{R}^q$  is the open set of all possible computer model parameter settings with an integer  $q \geq 1$ . Let  $\{\boldsymbol{\theta}_1, \dots, \boldsymbol{\theta}_p\} \subset \boldsymbol{\Theta}$  be a collection of  $p$  design points in the parameter space and  $\{\mathbf{s}_1, \dots, \mathbf{s}_n\} \subset \mathcal{S}$  be the set of  $n$  model grid locations.  $\mathbf{Y}_i = (Y(\mathbf{s}_1, \boldsymbol{\theta}_i), \dots, Y(\mathbf{s}_n, \boldsymbol{\theta}_i))^T$  is computer model output at the model grid locations at the parameter setting  $\boldsymbol{\theta}_i$ . The concatenated  $np \times 1$  vector of all computer model outputs is  $\mathbf{Y} = (\mathbf{Y}_1^T, \dots, \mathbf{Y}_p^T)^T$ . Note that typically  $p \ll n$  since computer model runs with high-resolution are computationally expensive. Finally, we let  $Z(\mathbf{s})$  be an observation at spatial location  $\mathbf{s}$  and  $\mathbf{Z} = (Z(\mathbf{s}_1), \dots, Z(\mathbf{s}_n))^T$  be the observational data, a spatial process observed at  $n$  locations.

**Model Emulation Using Gaussian Processes.** Following Bhat et al. (2012) and Chang et al. (2013), we construct a Gaussian process that interpolates computer model outputs as follows

$$\mathbf{Y} \sim N(\mathbf{X}\boldsymbol{\beta}, \Sigma(\boldsymbol{\xi}_y)),$$

where  $\mathbf{X}$  is an  $np \times b$  covariate matrix containing all the spatial locations and climate parameters (that is,  $\mathbf{s}_1, \dots, \mathbf{s}_n$  and  $\boldsymbol{\theta}_1, \dots, \boldsymbol{\theta}_p$ ) used to define the covariance matrix  $\Sigma(\boldsymbol{\xi}_y)$ .  $\boldsymbol{\beta}$  and  $\boldsymbol{\xi}_y$  are the vectors of regression coefficients and covariance parameters respectively. We construct an interpolation process by finding the maximum likelihood estimate (MLE) of these parameters. This interpolation model provides the predictive distribution of a computer model run at any given location  $\mathbf{s} \in \mathcal{S}$  and  $\boldsymbol{\theta} \in \boldsymbol{\Theta}$  (Sacks et al., 1989). We call this predictive process an emulator and denote it by  $\eta(\mathbf{s}, \boldsymbol{\theta})$ . Note that, throughout this paper,  $\boldsymbol{\beta}$  is set to be  $\mathbf{0}$  since the Gaussian process provides enough flexibility in modeling the output process.

**Model Calibration Using Gaussian Random Processes.** We model the observational data  $\mathbf{Z}$  by the following model,

$$\mathbf{Z} = \boldsymbol{\eta}(\boldsymbol{\theta}^*) + \boldsymbol{\delta}, \quad (1)$$

where  $\boldsymbol{\theta}^*$  is the true or fitted value of computer model parameter for the observational data (Bayarri et al., 2007),  $\boldsymbol{\eta}(\boldsymbol{\theta}^*) = (\eta(\mathbf{s}_1, \boldsymbol{\theta}^*), \dots, \eta(\mathbf{s}_n, \boldsymbol{\theta}^*))^T$  is the emulator output at  $\boldsymbol{\theta}^*$  on the model grid, and  $\boldsymbol{\delta} = (\delta(\mathbf{s}_1), \dots, \delta(\mathbf{s}_n))^T$  is a term that includes both data-model discrepancy as well as observational error. The discrepancy process  $\delta(\mathbf{s})$  is also modeled as a Gaussian process with spatial covariance between the locations  $\mathbf{s}_1, \dots, \mathbf{s}_n$ . Model calibration with high-dimensional spatial data leads to computational challenges as described in the following section.

### 3 Calibration with High-Dimensional Spatial Data

In this section we briefly examine the challenges in model calibration using high-dimensional spatial data and the existing approaches to the problem. We then proceed to the formulation of our composite likelihood approach.

#### 3.1 Challenges with High-Dimensional Spatial Data

The basic challenge with the approach in Section 2 stems from the fact that the computational cost for a single likelihood evaluation is  $\mathcal{O}(n^3 p^3)$ . For large  $n$ , evaluating the likelihood function repeatedly when using algorithms like Markov chain Monte Carlo (MCMC) can become computationally prohibitive. One can reduce the computational cost by assuming a separable covariance structure between the spatial dependence and the dependence due to computer model parameters, but the computational cost is still  $\mathcal{O}(n^3)$ , and hence does not scale well with  $n$ . The current approaches to overcome such limitation for high-dimensional data rely on dimension reduction or basis expansion. The dimension reduction approaches (Bayarri et al., 2007; Chang et al., 2013) map the original output into a lower dimension and exploit the uncorrelated nature of the low-

dimensional processes to speed up the computation. The basis expansion approaches (Bhat et al., 2012; Higdon et al., 2008) use a basis representation of model output that results in a reformulated likelihood with a lower computational cost. Here we introduce a somewhat different approach that relies on the block composite likelihood for spatial data (Caragea and Smith, 2006; Eidsvik et al., 2013).

### 3.2 Composite Likelihood for Model Calibration

In this framework, we partition the spatial field  $\mathcal{S}$  into small blocks to avoid the computational issues related to high-dimensional data. In Section 4 we describe an example of how such a partition may be constructed in practice. The block composite likelihood method substitutes the original likelihood by a composite likelihood that utilizes the spatial blocks, thereby resulting in a likelihood function that requires much less computational effort. In particular, we adopt the block composite likelihood formulation by Caragea and Smith (2006). This framework assumes conditional independence between outcomes in different blocks given the block means, and the dependence between blocks is modeled through the covariance between block means. Note that this framework gives a valid probability model, and therefore the posterior distribution defined using the composite likelihood function based on this approach is also a valid probability model. Obtaining a valid probability model is important because we are embedding the likelihood within a Bayesian approach; having a valid probability model automatically assures us that the resulting posterior distribution is proper when all the prior distributions used are proper.

We divide the spatial area for the computer model output into  $M$  different blocks and denote the output for each block by  $\mathbf{Y}_{(1)}, \dots, \mathbf{Y}_{(M)}$ . Note that the blocks are made according to the spatial field, not the parameter space, because the number of computer model runs is usually quite limited due to the high computational costs of running the model. However, in principle our approach may be extended to blocking in parameter space as well if the number of model runs is also large. Let  $n_i$  denote the number of computer model outcomes in the  $i$ th block. We denote the spatial locations in the  $i$ th

block by  $\mathbf{s}_{i1}, \dots, \mathbf{s}_{in_i}$ . Each  $\mathbf{Y}_{(i)}$  is a stack of  $(n_i - 1)$ -dimensional spatial output for  $p$  different parameter settings;

$$\mathbf{Y}_{(i)} = (Y(\mathbf{s}_{i1}, \cdot)^T, Y(\mathbf{s}_{i2}, \cdot)^T, \dots, Y(\mathbf{s}_{in_i-1}, \cdot)^T)^T,$$

141 where  $Y(\mathbf{s}_{ij}, \cdot) = (Y(\mathbf{s}_{ij}, \boldsymbol{\theta}_1), \dots, Y(\mathbf{s}_{ij}, \boldsymbol{\theta}_p))^T$  is the  $p \times 1$  vector of computer model out-  
 142 comes for all the parameter settings  $\boldsymbol{\theta}_1, \dots, \boldsymbol{\theta}_p$ . Note that we omit one spatial loca-  
 143 tion for each block in defining the output vectors to avoid degeneracy. We let  $\bar{\mathbf{Y}}_{(i)} =$   
 144  $\frac{1}{n_i} \sum_{j=1}^{n_i} (Y(\mathbf{s}_{ij}, \boldsymbol{\theta}_1), \dots, Y(\mathbf{s}_{ij}, \boldsymbol{\theta}_p))^T$  be the  $p$ -dimensional mean vector of model outcomes  
 145 for the  $i$ th block. That is, means for the spatial block consisting of same set of loca-  
 146 tions across all model parameter settings. We define the vector of all block means by  
 147  $\bar{\mathbf{Y}} = (\bar{\mathbf{Y}}_{(1)}^T, \dots, \bar{\mathbf{Y}}_{(M)}^T)^T$ . Similarly, we divide the observational data into  $M$  blocks in  
 148 the same way and omit one observation for each block to have  $\mathbf{Z}_{(1)}, \dots, \mathbf{Z}_{(M)}$ , the vectors  
 149 of observational data in different blocks. We let  $\bar{\mathbf{Z}}_{(i)} = \frac{1}{n_i} \sum_{j=1}^{n_i} Z(\mathbf{s}_{ij})$  be the  $i$ th block  
 150 mean of observational data and  $\bar{\mathbf{Z}} = (\bar{\mathbf{Z}}_{(1)}, \dots, \bar{\mathbf{Z}}_{(M)})^T$  be the collection of them.

Assuming separability, we model the covariance between the process at two different spatial locations and parameter settings  $Y(\mathbf{s}, \boldsymbol{\theta})$  and  $Y(\mathbf{s}', \boldsymbol{\theta}')$  by

$$\text{Cov}(Y(\mathbf{s}, \boldsymbol{\theta}), Y(\mathbf{s}', \boldsymbol{\theta}')) = K_s(\mathbf{s}, \mathbf{s}'; \boldsymbol{\xi}_s) K_\theta(\boldsymbol{\theta}, \boldsymbol{\theta}'; \boldsymbol{\xi}_\theta),$$

where  $K_s$  and  $K_\theta$  are valid covariance functions respectively in  $\mathcal{S}$  and  $\boldsymbol{\Theta}$  with parameters  $\boldsymbol{\xi}_s$  and  $\boldsymbol{\xi}_\theta$ . The covariance between discrepancy process  $\mathbf{s}$  and  $\mathbf{s}'$  is given by

$$\text{Cov}(\delta(\mathbf{s}), \delta(\mathbf{s}')) = K_d(\mathbf{s}, \mathbf{s}'; \boldsymbol{\xi}_d)$$

151 with a valid covariance function  $K_d$  in  $\mathcal{S}$  and a vector of parameters  $\boldsymbol{\xi}_d$ . More specific  
 152 definition of the covariance functions will be discussed below.

**Computer Model Emulation.** The first component of our composite likelihood is the model for block means, which captures the large scale trend. The covariance between

the block means is

$$\Sigma^{\bar{\mathbf{Y}}} = \mathbf{H} \otimes \Sigma_{\theta},$$

where  $\Sigma_{\theta}$  is the covariance matrix for the random variable across  $p$  parameter settings and  $\mathbf{H}$  is the  $M \times M$  covariance matrix between the blocks. It is straightforward to see that the block covariance is

$$\{\mathbf{H}\}_{ij} = \frac{1}{n_i n_j} \sum_{k=1}^{n_i} \sum_{l=1}^{n_j} K_s(\mathbf{s}_{ik}, \mathbf{s}_{jl}; \boldsymbol{\xi}_s), \quad (2)$$

the mean of all possible cross covariances between two blocks.

The second component is the sum of the conditional likelihoods for each block, which models the small scale dependence and variation. For the  $i$ th block, the conditional distribution of output  $\mathbf{Y}_{(i)}$  given the block mean  $\bar{\mathbf{Y}}_{(i)}$  is a normal distribution with the mean and covariance given by

$$\begin{aligned} \mu_i^{\mathbf{Y}|\bar{\mathbf{Y}}} &= E(\mathbf{Y}_{(i)}|\bar{\mathbf{Y}}_{(i)}) = (\gamma^{(i)} / \{\mathbf{H}\}_{ii} \otimes I_p) \bar{\mathbf{Y}}_{(i)} \\ \Sigma_i^{\mathbf{Y}|\bar{\mathbf{Y}}} &= Var(\mathbf{Y}_{(i)}|\bar{\mathbf{Y}}_{(i)}) = (\Gamma_i - \gamma^{(i)} (\gamma^{(i)})^T / \{\mathbf{H}\}_{ii}) \otimes \Sigma_{\theta} \end{aligned}$$

where

$$\begin{aligned} \{\gamma^{(i)}\}_j &= \sum_{k=1}^{n_i} K_s(\mathbf{s}_{ij}, \mathbf{s}_{ik}; \boldsymbol{\xi}_s) / n_i, \quad j = 1, \dots, n_i - 1, \\ \{\Gamma_i\}_{jk} &= K_s(\mathbf{s}_{ij}, \mathbf{s}_{ik}; \boldsymbol{\xi}_s), \quad j = 1, \dots, n_i - 1, \quad k = 1, \dots, n_i - 1. \end{aligned}$$

Here,  $\Gamma_i$  is the spatial covariance matrix for the  $i$ th block and  $\gamma^{(i)}$  is the  $(n_i - 1) \times 1$  covariance vector between the  $i$ th block mean and the  $i$ th block locations. The log composite likelihood function for the model output is then

$$\begin{aligned} cl(\boldsymbol{\xi}_s, \boldsymbol{\xi}_{\theta}) &\propto - \frac{1}{2} \left( \log |\Sigma^{\bar{\mathbf{Y}}}| + \bar{\mathbf{Y}}^T (\Sigma^{\bar{\mathbf{Y}}})^{-1} \bar{\mathbf{Y}} \right) \\ &- \frac{1}{2} \sum_{i=1}^M \left( \log |\Sigma_i^{\mathbf{Y}|\bar{\mathbf{Y}}}| + (\mathbf{Y}_{(i)} - \mu_i^{\mathbf{Y}|\bar{\mathbf{Y}}})^T (\Sigma_i^{\mathbf{Y}|\bar{\mathbf{Y}}})^{-1} (\mathbf{Y}_{(i)} - \mu_i^{\mathbf{Y}|\bar{\mathbf{Y}}}) \right), \end{aligned}$$



165 We construct the emulator by finding the MLE of  $\boldsymbol{\xi}_\theta$  and  $\boldsymbol{\xi}_s$ , denoted by  $\hat{\boldsymbol{\xi}}_\theta$  and  $\hat{\boldsymbol{\xi}}_s$ .  
 166 The computational cost for a single likelihood evaluation is reduced from  $\frac{1}{3}n^3$  flops to  
 167  $\sum_{i=1}^M \sum_{j=i}^M n_i n_j + \frac{1}{3}(M^3) + \frac{1}{3} \left( \sum_{i=1}^M (n_i - 1)^3 \right)$  flops, where the first term is the computa-  
 168 tional cost for finding H. This is a reduction from  $6.86 \times 10^{10}$  flops to  $5.92 \times 10^7$  flops in  
 169 the climate model calibration example in Section 4.

170 **Computer Model Calibration.** We formulate the composite likelihood for observa-  
 171 tional data in the same manner as above. Let  $\Omega$  be the  $M \times M$  covariance between the  
 172  $M$  block means of the discrepancy  $\boldsymbol{\delta}$ , defined in the same way as H with a different set of  
 173 parameters  $\boldsymbol{\xi}_d$ . The conditional mean and covariance for the block means of observational  
 174 data  $\bar{\mathbf{Z}}$  are

$$\begin{aligned}\mu^{\bar{\mathbf{Z}}} &= (I_M \otimes \Sigma_{\theta^* \theta} \Sigma_\theta^{-1}) \bar{\mathbf{Y}}, \text{ an } M \times 1 \text{ vector,} \\ \Sigma^{\bar{\mathbf{Z}}} &= H \otimes (\Sigma_{\theta^*} - \Sigma_{\theta^* \theta} \Sigma_\theta^{-1} \Sigma_{\theta^* \theta}^T) + \Omega, \text{ an } M \times M \text{ matrix.}\end{aligned}$$

175 Likewise, we define  $\Lambda_i$  and  $\lambda^{(i)}$  as the discrepancy counterparts of  $\Gamma_i$  and  $\gamma^{(i)}$  with the  
 176 covariance parameter  $\boldsymbol{\xi}_d$ . Hence,  $\Lambda_i$  and  $\lambda^{(i)}$  are the  $i$ th block discrepancy covariance  
 177 matrix and the  $(n_i - 1) \times 1$  covariance vector between the block outputs and the block  
 178 mean respectively,

$$\begin{aligned}\{\lambda^{(i)}\}_j &= \sum_{k=1}^{n_i} K_d(\mathbf{s}_{ij}, \mathbf{s}_{ik}; \boldsymbol{\xi}_d) / n_i, \quad j = 1, \dots, n_i - 1, \\ \{\Lambda_i\}_{jk} &= K_d(\mathbf{s}_{ij}, \mathbf{s}_{ik}; \boldsymbol{\xi}_d), \quad j = 1, \dots, n_i - 1, \quad k = 1, \dots, n_i - 1.\end{aligned}$$

179 The conditional mean and covariance for observational data in the  $i$ th block are therefore

$$\begin{aligned}\mu_i^{\mathbf{Z}|\bar{\mathbf{Z}}} &= (\mathbf{I}_{n_i-1} \otimes \Sigma_{\theta^* \theta} \Sigma_\theta^{-1}) \mathbf{Y}_{(i)} + (\tau^{(i)} + \lambda^{(i)}) \left\{ \Sigma^{\bar{\mathbf{Z}}} \right\}_{ii}^{-1} (\bar{\mathbf{Z}}_i - \left\{ \mu^{\bar{\mathbf{Z}}} \right\}_i), \\ \Sigma_i^{\mathbf{Z}|\bar{\mathbf{Z}}} &= (\Gamma_i \otimes (\Sigma_{\theta^*} - \Sigma_{\theta^* \theta} \Sigma_\theta^{-1} \Sigma_{\theta^* \theta}^T) + \Lambda_i) - (\tau^{(i)} + \lambda^{(i)}) (\tau^{(i)} + \lambda^{(i)})^T / \left\{ \Sigma^{\bar{\mathbf{Z}}} \right\}_{ii},\end{aligned}$$

180 where  $\tau^{(i)} = \gamma^{(i)} \otimes (\Sigma_{\theta^*} - \Sigma_{\theta^* \theta} \Sigma_\theta^{-1} \Sigma_{\theta^* \theta}^T)$ . The log composite likelihood for the observa-

181 tional data is then

$$\begin{aligned}
c\ell_n(\boldsymbol{\psi}) \propto & -\frac{1}{2} \left( \log |\Sigma^{\bar{\mathbf{Z}}}| + (\bar{\mathbf{Z}} - \mu^{\bar{\mathbf{Z}}})^T (\Sigma^{\bar{\mathbf{Z}}})^{-1} (\bar{\mathbf{Z}} - \mu^{\bar{\mathbf{Z}}}) \right) \\
& - \frac{1}{2} \sum_{i=1}^M \left( \log |\Sigma_i^{\mathbf{Z}|\bar{\mathbf{Z}}}| + (\mathbf{z}_{(i)} - \mu_i^{\mathbf{Z}|\bar{\mathbf{Z}}})^T (\Sigma_i^{\mathbf{Z}|\bar{\mathbf{Z}}})^{-1} (\mathbf{z}_{(i)} - \mu_i^{\mathbf{Z}|\bar{\mathbf{Z}}}) \right),
\end{aligned} \tag{3}$$

182 where the first line in (3) is the log likelihood corresponding to the block means and  
183 the second line corresponding to the observations within each block.  $\boldsymbol{\psi}$  denotes all the  
184 parameters being estimated in the calibration stage including  $\boldsymbol{\theta}^*$  and  $\boldsymbol{\xi}_d$ . By choosing a  
185 proper prior for  $\boldsymbol{\psi}$ ,  $f(\boldsymbol{\psi})$ , we define the approximate log posterior density,  $\log(\pi_n(\boldsymbol{\psi})) \propto$   
186  $\log f(\boldsymbol{\psi}) + c\ell_n(\boldsymbol{\psi})$  and infer  $\boldsymbol{\psi}$  using the standard Metropolis-Hastings algorithm. We  
187 allow the scale parameters for the emulator to be re-estimated along with the other  
188 parameters but fix the other emulator parameters in  $\boldsymbol{\xi}_s$  at their estimated values from  
189 the emulation stage (Bayarri et al., 2007; Bhat et al., 2012; Chang et al., 2013). The  
190 formulation results in the same computation gain as in the emulation stage.

191 In both the emulation and calibration stages, calculation of the covariance matrix  
192 for the block means is a computational bottleneck, requiring  $\sum_{i=1}^M \sum_{j=i}^M n_i n_j$  flops of  
193 computation. While computationally very demanding, its contribution to the likelihood  
194 function is usually not significant (Caragea and Smith, 2006). Therefore, instead of using  
195 all cross covariances between spatial locations, we randomly sample a subset of cross  
196 covariances to approximate the covariance between block means  $\mathbf{H}$ . The computation of  
197  $\mathbf{H}$  in (2) is substituted by

$$\{\mathbf{H}\}_{ij} = \frac{1}{m_i m_j} \sum_{k=1}^{m_i} \sum_{l=1}^{m_j} K_s(\mathbf{u}_{ik}, \mathbf{u}_{jl}; \boldsymbol{\xi}_s), \tag{4}$$

198 with  $m_i \leq n_i$  and  $m_j \leq n_j$ , where  $\mathbf{u}_{i1}, \dots, \mathbf{u}_{im_i}$  and  $\mathbf{u}_{j1}, \dots, \mathbf{u}_{jm_j}$  are randomly chosen  
199 respectively from  $\mathbf{s}_{i1}, \dots, \mathbf{s}_{in_i}$  and  $\mathbf{s}_{j1}, \dots, \mathbf{s}_{jn_j}$ . This reduces the computational cost from  
200  $\sum_{i=1}^M \sum_{j=i}^M n_i n_j$  to  $\sum_{i=1}^M \sum_{j=i}^M m_i m_j$ , that is,  $1.32 \times 10^7$  flops to  $2.86 \times 10^5$  flops for the  
201 calibration problem in Section 4. The same approximation can be applied to  $\Omega$  with  $\boldsymbol{\xi}_d$ .

**Covariance Function and Prior Specification.** We use the exponential covariance function to define the covariance between parameter settings ( $K_\theta$ ), spatial covariance for

the emulator ( $K_s$ ), and the spatial covariance for the discrepancy ( $K_d$ ) with a nugget term. To be more specific, the covariance between the process at two parameter settings  $\boldsymbol{\theta} = (\theta_1, \dots, \theta_q)^T$  and  $\boldsymbol{\theta}' = (\theta'_1, \dots, \theta'_q)^T$  is defined by

$$K_{\theta}(\boldsymbol{\theta}, \boldsymbol{\theta}'; \boldsymbol{\xi}_{\theta}) = \zeta_{\theta} 1(\boldsymbol{\theta} = \boldsymbol{\theta}') + \kappa_{\theta} \exp \left( - \sum_{i=1}^q \phi_{\theta,i} |\theta_i - \theta'_i| \right),$$

where  $\boldsymbol{\xi}_{\theta} = (\zeta_{\theta}, \kappa_{\theta}, \phi_{\theta,1}, \dots, \phi_{\theta,q})$ , and  $\zeta_{\theta}, \kappa_{\theta}, \phi_{\theta,1}, \dots, \phi_{\theta,q} > 0$ . Likewise, the covariance between the process at two spatial locations  $\mathbf{s}$  and  $\mathbf{s}'$  for the emulator and the discrepancy term are given by

$$K_s(\mathbf{s}, \mathbf{s}'; \boldsymbol{\xi}_s) = \kappa_s (\zeta_s 1(\mathbf{s} = \mathbf{s}') + \exp(-\phi_s g(\mathbf{s}, \mathbf{s}'))),$$

and

$$K_d(\mathbf{s}, \mathbf{s}'; \boldsymbol{\xi}_d) = \kappa_d (\zeta_d 1(\mathbf{s} = \mathbf{s}') + \exp(-\phi_d g(\mathbf{s}, \mathbf{s}'))), \quad (5)$$

respectively, with  $\boldsymbol{\xi}_s = (\zeta_s, \kappa_s, \phi_s)$ ,  $\boldsymbol{\xi}_d = (\zeta_d, \kappa_d, \phi_d)$ , and  $\zeta_s, \kappa_s, \phi_s, \zeta_d, \kappa_d, \phi_d > 0$ .  $g(\mathbf{s}, \mathbf{s}')$  denotes the distance between two points. In the climate model calibration problem in Section 4, for example,  $g$  is the geodesic distance between two points on the earth's surface.

The parameters inferred by the Bayesian approach in the calibration stage are  $\kappa_s$ ,  $\zeta_d$ ,  $\kappa_d$ ,  $\phi_d$ , and  $\boldsymbol{\theta}^*$ . Following Bayarri et al. (2007), the sill parameter for the emulator  $\kappa_s$  is initially inferred via maximum likelihood estimate in the emulation stage and re-estimated by Bayesian inference in the calibration stage. We impose informative priors on the above parameters to avoid potentially obtaining improper posterior distributions (cf. Berger et al., 2001) and identifiability issues. The latter is explained further in Section 4. The sill parameters,  $\kappa_s$  and  $\kappa_d$  receive inverse-Gamma priors  $IG(a_{\kappa_s}, b_{\kappa_s})$  and  $IG(a_{\kappa_d}, b_{\kappa_d})$ . We also impose an Inverse-Gamma prior  $IG(a_{\zeta_d}, b_{\zeta_d})$  for the nugget parameter  $\zeta_d$ . The prior density for the range parameter  $\phi_d$  is assumed to be uniform with a wide support. The fitted computer model parameter  $\boldsymbol{\theta}^*$  also receives a uniform

220 prior over a wide range. Note that one can also assume a more informative prior for  
 221  $\boldsymbol{\theta}^*$  such as a unimodal distribution based on some physical knowledge. However, in the  
 222 calibration problem in Section 4 we do not impose such a prior for  $\boldsymbol{\theta}^*$ ; this allows us to  
 223 study the characteristics of the posterior density of  $\boldsymbol{\theta}^*$  more transparently.

224 **Asymptotics and Adjustment using Godambe Information.** Note that the com-  
 225 posite likelihood in (3) is not based on the true probability model in (1), and therefore the  
 226 ‘composite’ posterior density based on (3) is quite different from the true posterior based  
 227 on (1). In this section, we will discuss how the Godambe information matrix (Godambe,  
 228 1960) for estimating equations may be used to adjust for using the composite likelihood  
 229 when making inferences.

We first provide the asymptotic justification for the adjustment using the Godambe  
 information matrix. We will show that, for large  $n$  and  $p$ , the mode of the approximate  
 posterior  $\hat{\boldsymbol{\psi}}_n^B = \arg \max_{\boldsymbol{\psi}} \pi_n(\boldsymbol{\psi})$  is consistent and asymptotically normally distributed  
 with a covariance matrix given by the inverse of the Godambe information matrix. If we  
 let  $p \rightarrow \infty$ , then the emulator converges to the measurement-error model such that

$$\boldsymbol{\eta}(\boldsymbol{\theta}) \sim N(\mathbf{Y}(\boldsymbol{\theta}), \zeta_{\boldsymbol{\theta}} \Sigma^s),$$

230 where  $\mathbf{Y}(\boldsymbol{\theta})$  is the  $n \times 1$  vector of model output at the parameter setting  $\boldsymbol{\theta}$  and the  
 231 spatial locations  $\mathbf{s}_1, \dots, \mathbf{s}_n$ . This result holds as long as the computer model output  
 232 varies reasonably smoothly in the parameter space (Yakowitz and Szidarovszky, 1985).  
 233 The model for observational data becomes

$$\mathbf{Z} \sim N(\mathbf{Y}^*, \zeta_{\boldsymbol{\theta}} \Sigma^s + \Sigma^d), \quad (6)$$

234 where  $\mathbf{Y}^* = \mathbf{Y}(\boldsymbol{\theta}^*)$ . The composite likelihood in (3) then has the following means and  
 235 covariances,

$$\begin{aligned} \mu^{\bar{\mathbf{Z}}} &= \bar{\mathbf{Y}}^*, \text{ an } M \times 1 \text{ vector,} \\ \Sigma^{\bar{\mathbf{Z}}} &= \zeta_{\boldsymbol{\theta}} \mathbf{H} + \Omega, \text{ an } M \times M \text{ matrix,} \end{aligned}$$

$$\begin{aligned}\mu_i^{\mathbf{Z}|\bar{\mathbf{Z}}} &= \mathbf{Y}_{(i)}^* + (\zeta_\theta \gamma^{(i)} + \lambda^{(i)}) \left\{ \Sigma^{\bar{\mathbf{Z}}} \right\}_{ii}^{-1} (\bar{\mathbf{Z}}_i - \left\{ \mu^{\bar{\mathbf{Z}}} \right\}_i), \\ \Sigma_i^{\mathbf{Z}|\bar{\mathbf{Z}}} &= (\zeta_\theta \Gamma_i + \Lambda_i) - (\zeta_\theta \gamma^{(i)} + \lambda^{(i)}) (\zeta_\theta \gamma^{(i)} + \lambda^{(i)})^T / \{ \Sigma^{\bar{\mathbf{Z}}} \}_{ii},\end{aligned}$$

where  $\bar{\mathbf{Y}}_{(i)}^* = \frac{1}{n_i} \sum_{j=1}^{n_i} Y(\mathbf{s}_{ij}, \boldsymbol{\theta}^*)$  is the  $i$ th block mean of the computer model output at  $\boldsymbol{\theta}^*$  and  $\bar{\mathbf{Y}}^* = \left( \bar{\mathbf{Y}}_{(1)}^*, \dots, \bar{\mathbf{Y}}_{(M)}^* \right)^T$  is the collection of all their block means.

We now show the consistency and the asymptotic normality of the posterior mode  $\hat{\boldsymbol{\psi}}_n^B$  as  $n \rightarrow \infty$ . We utilize expanding domain asymptotic results (see e.g. Mardia and Marshall, 1984; Cressie, 1993; Cox and Reid, 2004; Zhang and Zimmerman, 2005; Varin, 2008). The first step is establishing consistency and asymptotic normality of the maximum composite likelihood estimator.

**Proposition 1.** *The following holds for the maximum composite likelihood estimator*

$$\hat{\boldsymbol{\psi}}_n^{CL} = \arg \max_{\boldsymbol{\psi}} \text{cl}_n(\boldsymbol{\psi});$$

(i) (Consistency) *The maximum composite likelihood estimator is consistent for  $\boldsymbol{\psi}^0$ ;*

$$\hat{\boldsymbol{\psi}}_n^{CL} \xrightarrow{\mathcal{P}} \boldsymbol{\psi}^0,$$

as  $n \rightarrow \infty$ , where  $\boldsymbol{\psi}^0$  is the vector of true values of parameters in  $\boldsymbol{\psi}$ .

(ii) (Asymptotic Normality) *The asymptotic distribution of the maximum composite likelihood estimator is given by*

$$\mathbf{G}_n^{\frac{1}{2}} \left( \hat{\boldsymbol{\psi}}_n^{CL} - \boldsymbol{\psi}^0 \right) \xrightarrow{\mathcal{D}} N(0, \mathbf{I}),$$

where  $\mathbf{G}_n = \mathbf{Q}_n \mathbf{P}_n^{-1} \mathbf{Q}_n$  is the Godambe information matrix (Godambe, 1960).  $\mathbf{P}_n$  is the covariance matrix of the gradient  $\nabla \text{cl}_n$  and  $\mathbf{Q}_n$  is the negative expected value of the Hessian matrix of  $\text{cl}_n$ , where both are evaluated at  $\boldsymbol{\psi} = \boldsymbol{\psi}^0$ .

*Proof.* For a composite likelihood, it is sufficient to verify the same regularity conditions as for the usual maximum likelihood estimators (Lindsay, 1988). In the context of expanding domain asymptotics in spatial statistics, the spatial covariance function and its first and second derivatives need to be absolutely summable. From Theorem 3 in Mardia and

Marshall (1984), this condition holds for the exponential covariance function that we are using here. (i) and (ii) follow immediately.  $\square$

We are ready to state the main result of this section, which establishes the consistency and asymptotic normality of the posterior mode,  $\hat{\boldsymbol{\psi}}_n^B$ .

**Proposition 2.** (i) (*Posterior consistency*) The posterior degenerates on the true value  $\boldsymbol{\psi}^0$  in total variation, i.e.

$$|\pi_n(\boldsymbol{\psi}) - \pi_n^0(\boldsymbol{\psi})|_{TV} \xrightarrow{\mathcal{P}} 0 \quad (7)$$

as  $n \rightarrow \infty$  where  $|\cdot|_{TV}$  is the total variation norm and  $\pi_n^0(\boldsymbol{\psi})$  is a normal density with the mean  $\boldsymbol{\psi}^0 + \mathbf{Q}_n^{-1} \nabla \text{cl}_n(\boldsymbol{\psi}^0)$  and the covariance  $\mathbf{Q}_n^{-1}$ . Note that  $\mathbf{Q}_n^{-1} \rightarrow \mathbf{0}$  as  $n \rightarrow \infty$ .

(ii) (*Asymptotic normality*) The density of  $\hat{\boldsymbol{\psi}}_n^B$  is asymptotically normal;

$$\mathbf{G}_n^{\frac{1}{2}} \left( \hat{\boldsymbol{\psi}}_n^B - \boldsymbol{\psi}^0 \right) \xrightarrow{\mathcal{D}} N(0, \mathbf{I}), \quad (8)$$

as  $n \rightarrow \infty$ .

*Proof.* When the maximum composite likelihood estimator  $\boldsymbol{\psi}_n^{CL}$  is consistent and asymptotically normal, (i) and (ii) follow (Theorems 1 and 2 respectively in Chernozhukov and Hong, 2003). Hence the result follows directly from Proposition 1.  $\square$

**Application of Gobambe Adjustment.** We have several options for adjusting our composite likelihood-based inference. These include (a) direct use of the asymptotic distribution in (8); (b) ‘open-faced sandwich’ post-hoc adjustment (Shaby, 2012) of MCMC sample from the composite posterior distribution  $\pi_n(\boldsymbol{\psi})$ ; (c) ‘curvature’ adjustment (Coley et al., 2011) for our MCMC procedure. We will utilize (b) and (c) because these MCMC-based methods can capture the higher-order moments of the posterior distribution, which may be important in finite sample inference.

For any of these methods, it is necessary to evaluate  $\mathbf{P}_n$  and  $\mathbf{Q}_n$ . See the appendix for an example of their analytic computation. Note that  $\mathbf{Q}_n$  can also be obtained using MCMC runs from the posterior distribution  $\pi_n(\boldsymbol{\psi})$  by the asymptotic result in (7).

We caution that the adjustment procedures here rely on the identifiability of parameters in  $\boldsymbol{\psi}$ . In order to evaluate  $\mathbf{P}_n$  and  $\mathbf{Q}_n$  under the correct probability model in (6), we need to be able to estimate the true value  $\boldsymbol{\psi}^0$  accurately by the posterior mode  $\hat{\boldsymbol{\psi}}_n^B$ . This may not always hold as there is a trade-off between the discrepancy parameters in  $\boldsymbol{\xi}_d$  for finite sample sizes.

The open-faced sandwich adjustment is one approach for adjusting the covariance based on Proposition 2 (Shaby, 2012). For any MCMC sample of  $\boldsymbol{\psi}$  from  $\pi_n(\boldsymbol{\psi})$ , the open-faced sandwich adjustment is defined by  $\tilde{\boldsymbol{\psi}}^{open} = \hat{\boldsymbol{\psi}}_n^B + \mathbf{C}(\boldsymbol{\psi} - \hat{\boldsymbol{\psi}}_n^B)$  with  $\mathbf{C} = \mathbf{Q}_n^{-1} \mathbf{P}_n^{\frac{1}{2}} \mathbf{Q}_n^{\frac{1}{2}}$ . Similar to the curvature adjustment, this approach guarantees that the distribution of the adjusted posterior sample has the same posterior mode and the desired asymptotic covariance  $\mathbf{G}_n^{-1}$ . Note that this method can be either embedded in each step of MCMC run or applied after an entire MCMC run is finished.

Another approach is curvature adjustment (Cooley et al., 2011), which substitutes  $\boldsymbol{\psi}$  in (3) with  $\tilde{\boldsymbol{\psi}}^{curv} = \hat{\boldsymbol{\psi}}_n^B + \mathbf{D}(\boldsymbol{\psi} - \hat{\boldsymbol{\psi}}_n^B)$ , where  $\boldsymbol{\psi}$  is the posterior mode from (3).  $\mathbf{D}$  is the matrix that satisfies  $\mathbf{D}^T \mathbf{Q}_n \mathbf{D} = \mathbf{Q}_n \mathbf{P}_n^{-1} \mathbf{Q}_n$ . This approach ensures that the resulting posterior distribution has the same mode as the original composite likelihood  $c\ell_n(\boldsymbol{\psi})$  and the asymptotic covariance  $\mathbf{G}_n^{-1}$  as described in (8). Note that the choice for  $\mathbf{D}$  is not unique, and Cooley et al. (2011) suggested using  $\mathbf{D} = \mathbf{Q}_n^{\frac{1}{2}} (\mathbf{Q}_n \mathbf{P}_n^{-1} \mathbf{Q}_n)^{\frac{1}{2}}$  where the square roots of the matrices are computed using singular value decomposition. Here we use the open-faced adjustment; the curvature adjustment approach may also be used but, as shown in (Shaby, 2012), the difference between the two approaches is likely to be minimal.

## 4 Application to UVic ESCM Calibration

We demonstrate the application of our approach to a climate model calibration problem. The computer model used here is the University of Victoria Earth system climate model (UVic ESCM) of intermediate complexity (Weaver et al., 2001). The input parameter that we are interested in is climate sensitivity (CS), defined as the equilibrium global

mean surface air temperature change due to a doubling of carbon dioxide concentrations in the atmosphere (Andronova et al., 2007; Knutti and Hegerl, 2008). Climate sensitivity is an important model diagnostic and used as an input to climate projections as well as economic assessments of climate change impacts (see e.g. Nordhaus and Boyer, 2000; Keller et al., 2004). Each model run is a spatial pattern of ocean temperature anomaly on a regular  $1.8^\circ$  latitude by  $3.6^\circ$  longitude grid, defined as change between 1955-1964 mean and 2000-2009 mean in degree Celsius times meter ( $^\circ\text{C m}$ ). At each location, the ocean temperature anomaly is vertically integrated from 0 to 2000 m. in depth.

Note that the model output has regions of missing data since it covers only the ocean, and partition of the spatial area needs careful consideration. We partition the spatial area using a random tessellation; this is also the approach followed by Eidsvik et al. (2013). We first randomly choose  $M$  different centroids out of total  $n$  locations and then assign the spatial locations to different subregions according to the nearest centroid in terms of geodesic distance. When finding the nearest centroid for each point, we only consider the centroids in the same ocean to avoid assigning locations separated by land to the same block. This random tessellation ensures, on average, that we have more subregions where data points are more densely distributed.

## 4.1 Simulated Examples

We conducted some perfect model experiments to answer the following questions: (i) Is the posterior density based on the composite likelihood (composite posterior) similar to the posterior density based on the original likelihood (original posterior)? (ii) Is the posterior density with approximated block mean covariance computation (approximated composite posterior) described in (4) close to the true composite posterior? (iii) How do the number of spatial blocks and the magnitude of the discrepancy affect the composite posterior density?

Each experiment follows four key steps below:

1. Choose one of the parameter settings for model runs as the synthetic truth.



2. Leave the corresponding model run out and superimpose a randomly generated error on it to construct a synthetic observation.
3. Emulate the computer model using the remaining model runs.
4. Calibrate the computer model using the emulator in 3 and compare the resulting density with the synthetic truth.

To be able to compute the original posterior density with a reasonable computational effort, we restrict ourselves to a subset of spatial locations consisting of 1000 randomly selected points and assume separable covariance structure for the spatial field and the computer model parameter space. The synthetic truth for the climate sensitivity used here is 2.153, but choosing other parameter settings gives similar results shown here.

A comparison between the composite posterior densities with 10 blocks and the original posterior densities are shown in Figure 1(a) and 1(b). We used two different realizations of the model-observation discrepancy. These were generated from a Gaussian process model with exponential covariance (5) with  $\zeta_d^* = 0.01$ ,  $\kappa_d^* = 160000$ , and  $\phi_d^* = 690$  km, where  $(\zeta_d^*, \kappa_d^*, \phi_d^*)$  are assumed true values of  $(\zeta_d, \kappa_d, \phi_d)$ . We also conducted the same comparison for the approximated composite posterior densities (Figure 1(c) and 1(d)). The posterior densities and the resulting credible intervals from all three approaches are reasonably similar. The composite posterior densities after adjustment are slightly more dispersed than the original posterior due to the information loss caused by blocking, but the modes are quite close to the original ones confirming the consistency result in Proposition 2 (i).

We also compared the adjusted composite posterior densities with different numbers of blocks to examine the effect of the number of blocks on calibration results (Figure 2). The results show that using more than 30 blocks introduce a slight bias for the posterior mode which might be due to the reduced number of data points in each block. However, the credible intervals are again reasonably similar to each other. Similarly, we compare the adjusted composite posterior densities based on datasets generated using different assumed sill values,  $\kappa_d^* = 40000, 90000$  and  $160000$  to investigate the effect of magnitude

of discrepancy on calibration results (Figure 3). As one would expect, the posterior density becomes more dispersed as we increase the value of the sill.

We used informative priors for the statistical parameters, which is important to reduce the identifiability issues occurring in the calibration based on observational data in Section 4.2. We imposed a vague prior for the nugget parameter  $\zeta_d \sim IG(2, 0.01(2 + 1))$  and a highly informative prior for the sill parameter  $\kappa_d \sim IG(10000, \kappa_d^*(10000 + 1))$ . The sill parameter for the emulator  $\kappa_s$  is given a mildly informative prior with  $IG(20, \hat{\kappa}_s(20 + 1))$ , where  $\hat{\kappa}_s$  is the MLE of  $\kappa_s$  computed in the emulated stage. The shape parameters for the inverse-Gamma distributions are specified in the way that the prior modes are aligned with certain target values. Note that inference for simulated examples does not suffer from identifiability issues without the informative priors; we use these priors only to be consistent with the calibration based on observational data below.

## 4.2 Calibration using Observational Data

As an illustrative example, we calibrate the climate sensitivity using the observed spatial pattern of ocean temperature anomaly from the data product constructed by Levitus et al. (2012). We interpolated the observational data onto the UVic model grid using a simple bilinear interpolator. This step allows us to assume separability of emulation error and spatial covariance. We divide the 5,903 locations into 50 blocks using the random tessellation method described above. The covariance matrices for block means are approximated using (4) with  $m_i = \min(10, n_i)$  for  $i = 1, \dots, 50$ . The prior specification is the same as the simulated example with assumed sill ( $\kappa_d^*$ ) of 160,000, except that the discrepancy range parameter  $\phi_d$  is restricted to be greater than 800 km to reduce identifiability issues. Figure 4 shows the posterior density of climate sensitivity. The length of the MCMC chain is 15,000, and the computing time is about 15 hours (wall time) via parallel computing using 32 high-performance cores for a system with Intel Xeon E5450 Quad-Core 434 at 3.0 GHz. We verified that our MCMC algorithm and chain length were adequate by ensuring that the MCMC standard errors for our parameter estimates (Jones et al., 2006; Flegel et al., 2008) are small enough and by comparing posterior

density estimates after various run lengths to see that the results, namely posterior pdfs, have stabilized.

## 5 Discussion

### 5.1 Summary and future direction

This work is, to our knowledge, the first application of composite likelihood to the computer model calibration problem. Our composite likelihood approach enables computationally efficient inference in computer model calibration using high-dimensional spatial data. We proved consistency and asymptotic normality of our posterior estimates and established covariance adjustment for posterior density based on them. The adjustment can be easily integrated into common MCMC algorithms such as the Metropolis-Hastings algorithm. The block composite likelihood used here yields a valid probability model, and therefore no additional verification for the propriety of the posterior distribution is necessary.

An attractive benefit of this general framework is that it is relatively easy, in principle, to extend the approach to a more complicated and easy-to-interpret covariance model. For example, by allowing covariance parameters to vary across the different spatial blocks, our approach can introduce non-stationarity in the spatial processes of model output and observational data.

### 5.2 Caveats

While our approach is helpful in mitigating computational issues for various calibration problems, there is still more work to be done to make the computation more efficient. As  $n$  continues to get large the number of spatial locations in each block may become excessively large and evaluation of composite likelihood may not be computationally tractable. One may consider increasing the number of blocks until the computation becomes feasible, but then the convergence of the posterior modes may be very slow due to too small block sizes (Cox and Reid, 2004; Varin, 2008). Another perhaps simpler

approach is to use a composite likelihood framework that does not involve blocks though this may involve the need for analytical work to establish posterior propriety.

Another possible issue is related to the use of a Gaussian emulator in place of the true computer model in computing  $\mathbf{P}_n$  and  $\mathbf{Q}_n$ . Using a Gaussian process emulator, we approximate not only the true computer model itself, but also its first and second derivatives. In our particular example above, this does not cause any problem due to very regular behavior of the computer model output with respect to the input parameters. Note, however, that this may not be true in general and therefore  $\mathbf{P}_n$  and  $\mathbf{Q}_n$  calculations may be inaccurate.

It is also worth noting that the asymptotic independence between input parameters and discrepancy parameters does not usually hold in a finite sample. It is well known that calibration models usually suffer from identifiability issues (Wynn, 2001). One way to avoid the issues is imposing discrepancy prior information on the discrepancy term (Arendt et al., 2012) as we did in Section 4.

The scientific result shown in 4.2 requires some caution in its interpretation. First, besides climate sensitivity, climate system response to changes in radiatively active gases in the atmosphere also depends on the magnitude of the radiative effects of these gases (“radiative forcing”), and on the vertical mixing of heat into the deep ocean (Hansen et al., 1985; Knutti et al., 2002; Schmittner et al., 2009; Urban and Keller, 2010). The parameters controlling both the forcing, and the vertical mixing, were kept fixed in the model runs we use. Including these additional uncertainties is expected to make the posterior density of CS more dispersed. The example serves as a demonstration of computational feasibility of our approach when applied to high-dimensional spatial datasets rather than providing an improved estimate of CS. Second, the variability of the posterior density is very sensitive to the prior information for the discrepancy term. Note, however, that this is a common problem for many calibration problems as discussed earlier.

## Appendix: Computation of $\mathbf{P}_n$ and $\mathbf{Q}_n$ .

In this supplementary material, we describe the matrix computation for  $\mathbf{P}_n = \text{Cov} \left( c\dot{\ell}_n(\boldsymbol{\psi}) \right)$  and  $\mathbf{Q}_n = \text{E} \left( c\ddot{\ell}_n(\boldsymbol{\psi}) \right)$ . For ease of computation, it is useful to rewrite the composite likelihood function when  $p = \infty$  in the following way:

$$c\ell_n(\boldsymbol{\psi}) \propto -\frac{1}{2} \left( \log |\Sigma^{\bar{\mathbf{Z}}}| + (\bar{\mathbf{Z}} - \bar{\mathbf{Y}}^*)^T \left( \Sigma^{\bar{\mathbf{Z}}} \right)^{-1} (\bar{\mathbf{Z}} - \bar{\mathbf{Y}}^*) \right) \\ - \frac{1}{2} \left( \sum_{i=1}^M \log |\Sigma_i^{\mathbf{Z}|\bar{\mathbf{Z}}}| + \sum_{i=1}^M (\mathbf{Z}_{[i]} - \mathbf{Y}_{[i]}^*)^T \mathbf{A}_i^T \left( \Sigma_i^{\mathbf{Z}|\bar{\mathbf{Z}}} \right)^{-1} \mathbf{A}_i (\mathbf{Z}_{[i]} - \mathbf{Y}_{[i]}^*) \right),$$

where  $\mathbf{A}_i$  is a  $(n_i - 1) \times n_i$  matrix such that

$$\mathbf{A}_i = \left( \mathbf{I}_{(n_i-1) \times (n_i-1)} \mathbf{0}_{(n_i-1) \times 1} \right) - \mathbf{a}_i \left( \frac{1}{n_i}, \dots, \frac{1}{n_i} \right)_{1 \times n_i},$$

and  $\mathbf{a}_i$  is a  $(n_i - 1) \times 1$  vector such that

$$\mathbf{a}_i = \left( \zeta_{\theta} \gamma^{(i)} + \lambda^{(i)} \right) \left\{ \Sigma^{\bar{\mathbf{Z}}} \right\}_{ii}^{-1}.$$

$\mathbf{Z}_{[i]}$  is a  $n_i \times 1$  vector containing all the  $n_i$  observational data in the  $i$ th spatial block without omission, and  $\mathbf{Y}_{[i]}$  is a  $n_i \times 1$  vector of model output at  $\boldsymbol{\theta}^*$  defined in the same way. Omitting the part irrelevant to the data, the partial derivative of  $c\ell_n(\boldsymbol{\psi})$  with respect to the  $j$ th computer model parameter,  $\theta_j^*$ , is given by

$$\frac{\partial c\ell_n(\boldsymbol{\psi})}{\partial \theta_j^*} \propto \bar{\mathbf{B}}_j^* (\bar{\mathbf{Z}} - \bar{\mathbf{Y}}^*) + \sum_{i=1}^M \mathbf{B}_{i,j}^* (\mathbf{Z}_{[i]} - \mathbf{Y}_{[i]}^*),$$

436 where

$$\bar{\mathbf{B}}_j^* = \frac{\partial \bar{\mathbf{Y}}^*}{\partial \theta_j^*} \left( \Sigma^{\bar{\mathbf{Z}}} \right)^{-1}, \\ \mathbf{B}_{i,j}^* = \left( \frac{\partial \mathbf{Y}_{[i]}^*}{\partial \theta_j^*} \right)^T \mathbf{A}_i^T \left( \Sigma_i^{\mathbf{Z}|\bar{\mathbf{Z}}} \right)^{-1} \mathbf{A}_i.$$

437 We let  $\boldsymbol{\xi}$  be the vector containing all the parameters in  $\boldsymbol{\xi}_d$  as well as the emulator pa-  
 438 rameter being re-estimated. The partial derivative with respect to the  $k$ th parameter in  
 439  $\boldsymbol{\xi}$ ,  $\xi_k$ , can be written as

$$\begin{aligned} \frac{\partial \text{cl}_n(\boldsymbol{\psi})}{\partial \xi_k} &\propto \frac{1}{2}(\bar{\mathbf{Z}} - \bar{\mathbf{Y}}^*)^T \bar{\mathbf{B}}_k^d (\bar{\mathbf{Z}} - \bar{\mathbf{Y}}^*) \\ &+ \frac{1}{2} \sum_{i=1}^M (\mathbf{Z}_{[i]} - \mathbf{Y}_{[i]}^*)^T \mathbf{B}_{i,k}^d (\mathbf{Z}_{[i]} - \mathbf{Y}_{[i]}^*) \\ &+ \sum_{i=1}^M (\mathbf{Z}_{[i]} - \mathbf{Y}_{[i]}^*)^T \tilde{\mathbf{B}}_{i,k}^d (\mathbf{Z}_{[i]} - \mathbf{Y}_{[i]}^*) \end{aligned}$$

440 where

$$\begin{aligned} \bar{\mathbf{B}}_k^d &= \left( \Sigma^{\bar{\mathbf{Z}}} \right)^{-1} \frac{\partial \Sigma^{\bar{\mathbf{Z}}}}{\partial \xi_k} \left( \Sigma^{\bar{\mathbf{Z}}} \right)^{-1}, \\ \mathbf{B}_{i,k}^d &= \mathbf{A}_i^T \left( \Sigma_i^{\mathbf{Z}|\bar{\mathbf{Z}}} \right)^{-1} \frac{\partial \Sigma_i^{\mathbf{Z}|\bar{\mathbf{Z}}}}{\partial \xi_k} \left( \Sigma_i^{\mathbf{Z}|\bar{\mathbf{Z}}} \right)^{-1} \mathbf{A}_i, \\ \tilde{\mathbf{B}}_{i,k}^d &= - \left( \frac{\partial \mathbf{A}_i}{\partial \xi_k} \right)^T \left( \Sigma_i^{\mathbf{Z}|\bar{\mathbf{Z}}} \right)^{-1} \mathbf{A}_i. \end{aligned}$$

441 Note that inference on  $\boldsymbol{\theta}^*$ , our main goal, requires only calculating the asymptotic  
 442 covariance of  $\hat{\boldsymbol{\theta}}_n^B$  due to the asymptotic independence between  $\hat{\boldsymbol{\theta}}_n^B$  and  $\hat{\boldsymbol{\xi}}_n^B$ , the posterior  
 443 modes of  $\boldsymbol{\theta}^*$  and  $\boldsymbol{\xi}$  respectively. More specifically, for any  $j$  and  $k$ ,

$$\text{Cov} \left( \frac{\partial \text{cl}_n(\boldsymbol{\psi})}{\partial \theta_j^*}, \frac{\partial \text{cl}_n(\boldsymbol{\psi})}{\partial \xi_k} \right) = 0,$$

444 because a linear combinations of zero-mean normal random variables and a quadratic  
 445 form of the same variables are uncorrelated to one another. As a result,  $\hat{\boldsymbol{\theta}}_n^B$  and  $\hat{\boldsymbol{\xi}}_n^B$  have  
 446 zero cross-covariance in  $\mathbf{G}_n$  and are asymptotically independent due to normality. Let  $\mathbf{P}_n^*$   
 447 be a part of  $\mathbf{P}_n$ , which is the covariance matrix between partial derivatives with respect  
 448 to the parameters in  $\boldsymbol{\theta}^*$  only. Likewise, let  $\mathbf{Q}_n^*$  be a part of  $\mathbf{Q}_n$  that contains only the  
 449 negative expected Hessian of the parameters in  $\boldsymbol{\theta}^*$ . For inference on  $\boldsymbol{\theta}^*$ , it is sufficient to  
 450 compute  $\mathbf{P}_n^*$  and  $\mathbf{Q}_n^*$  instead of  $\mathbf{P}_n$  and  $\mathbf{Q}_n$ .

451 We compute the  $(k, l)$ th element of  $\mathbf{P}_n^*$  by plugging in  $\hat{\boldsymbol{\psi}}_n^B$  in place of  $\boldsymbol{\psi}$  in the following

452 expression:

$$\begin{aligned}
\text{Cov} \left( \frac{\partial c\ell_n(\boldsymbol{\psi})}{\partial \theta_k^*}, \frac{\partial c\ell_n(\boldsymbol{\psi})}{\partial \theta_l^*} \right) = & \quad \bar{\mathbf{B}}_k^* \Sigma^{\bar{\mathbf{Z}}} (\bar{\mathbf{B}}_l^*)^T \\
& + \sum_{i=1}^M \sum_{j=1}^M \mathbf{B}_{i,k}^* \Sigma_{i,j}^{\mathbf{Z}} (\mathbf{B}_{j,l}^*)^T \\
& + \sum_{i=1}^M \bar{\mathbf{B}}_k^* \Sigma_i^{\bar{\mathbf{Z}}, \mathbf{Z}} (\mathbf{B}_{i,l}^*)^T \\
& + \sum_{i=1}^M \bar{\mathbf{B}}_l^* \Sigma_i^{\bar{\mathbf{Z}}, \mathbf{Z}} (\mathbf{B}_{i,k}^*)^T,
\end{aligned}$$

453 where  $\Sigma_{i,j}^{\mathbf{Z}}$  is the  $n_i \times n_j$  covariance matrix between  $\mathbf{Z}_{[i]}$  and  $\mathbf{Z}_{[j]}$ , and  $\Sigma_i^{\bar{\mathbf{Z}}, \mathbf{Z}}$  is the  $1 \times n_i$   
454 covariance matrix between  $\bar{\mathbf{Z}}$  and  $\mathbf{Z}_{[i]}$  under the probability model in (3). Similarly, the  
455 second order partial derivative of  $c\ell_n(\boldsymbol{\psi})$  with respect to  $\theta_j^*$  and  $\theta_k^*$  is given by

$$\begin{aligned}
\frac{\partial^2 c\ell_n(\boldsymbol{\psi})}{\partial \theta_j^* \partial \theta_k^*} \propto & \quad \left( \frac{\partial^2 \bar{\mathbf{Y}}^*}{\partial \theta_j^* \partial \theta_k^*} \right)^T (\Sigma^{\bar{\mathbf{Z}}})^{-1} (\bar{\mathbf{Z}} - \bar{\mathbf{Y}}^*) \\
& - \left( \frac{\partial \bar{\mathbf{Y}}^*}{\partial \theta_j^*} \right)^T (\Sigma^{\bar{\mathbf{Z}}})^{-1} \frac{\partial \bar{\mathbf{Y}}^*}{\partial \theta_k^*} \\
& + \sum_{i=1}^M \left( \frac{\partial^2 \mathbf{Y}_{[i]}^*}{\partial \theta_j^* \partial \theta_k^*} \right)^T \mathbf{B}_i^T (\Sigma_i^{\mathbf{Z}|\bar{\mathbf{Z}}})^{-1} \mathbf{B}_i (\mathbf{Z}_{[i]} - \mathbf{Y}_{[i]}^*) \\
& - \sum_{i=1}^M \left( \frac{\partial \mathbf{Y}_{[i]}^*}{\partial \theta_j^*} \right)^T \mathbf{B}_i^T (\Sigma_i^{\mathbf{Z}|\bar{\mathbf{Z}}})^{-1} \mathbf{B}_i \frac{\partial \mathbf{Y}_{[i]}^*}{\partial \theta_k^*}.
\end{aligned}$$

456 The  $(j, k)$ th element of  $\mathbf{Q}_n^*$  is computed by substituting  $\boldsymbol{\psi}$  with  $\hat{\boldsymbol{\psi}}_n^B$  in the following  
457 equation:

$$\begin{aligned}
-E \left( \frac{\partial^2 c\ell_n(\boldsymbol{\psi})}{\partial \theta_j^* \partial \theta_k^*} \right) \propto & \quad \left( \frac{\partial \bar{\mathbf{Y}}^*}{\partial \theta_j^*} \right)^T (\Sigma^{\bar{\mathbf{Z}}})^{-1} \frac{\partial \bar{\mathbf{Y}}^*}{\partial \theta_k^*} \\
& + \sum_{i=1}^M \left( \frac{\partial \mathbf{Y}_{[i]}^*}{\partial \theta_j^*} \right)^T \mathbf{B}_i^T (\Sigma_i^{\mathbf{Z}|\bar{\mathbf{Z}}})^{-1} \mathbf{B}_i \frac{\partial \mathbf{Y}_{[i]}^*}{\partial \theta_k^*}.
\end{aligned}$$

458 Computing  $\mathbf{P}_n^*$  and  $\mathbf{Q}_n^*$  requires finding the first-order derivatives of  $\mathbf{Y}_{[1]}^*, \dots, \mathbf{Y}_{[M]}^*$ ,  
459 and  $\bar{\mathbf{Y}}^*$ . Since they are unknown functions of  $\boldsymbol{\theta}^*$ , we approximate them using the cor-  
460 responding derivatives of the emulator output. The approximated derivatives of  $\bar{\mathbf{Y}}^*$  and

461  $\mathbf{Y}_{[i]}^*$  with respect to  $\theta_j^*$  are given by

$$\begin{aligned}\frac{\partial \bar{\mathbf{Y}}^*}{\partial \theta_j^*} &= \left( I_M \otimes \left( \frac{\partial \Sigma_{\theta^* \theta}}{\partial \theta_j^*} \Sigma_{\theta}^{-1} \right) \right) \bar{\mathbf{Y}}, \\ \frac{\partial \mathbf{Y}_{[i]}^*}{\partial \theta_j^*} &= \left( I_{n_i} \otimes \left( \frac{\partial \Sigma_{\theta^* \theta}}{\partial \theta_j^*} \Sigma_{\theta}^{-1} \right) \right) \mathbf{Y}_{[i]}.\end{aligned}$$

The derivative term  $\frac{\partial \Sigma_{\theta^* \theta}}{\partial \theta_j^*}$  is determined by the covariance function for the parameter space. For the exponential covariance function used in our example, the derivative is

$$\left\{ \frac{\partial \Sigma_{\theta^* \theta}}{\partial \theta_i^*} \right\}_j = \phi_{\theta, i} (-1)^{1(\theta_i^* > \theta_{ij})} \exp \left( - \sum_{k=1}^q \phi_{\theta, k} |\theta_k^* - \theta_{kj}| \right), \quad i = 1, \dots, q, \quad j = 1, \dots, p,$$

462 where  $1(\cdot)$  is the indicator function, and  $\theta_{ij}$  is the  $i$ th parameter value of the  $j$ th design  
463 point  $\boldsymbol{\theta}_j$ .

464 **Acknowledgment** This work was partly supported by NSF through the Network  
465 for Sustainable Climate Risk Management (SCRiM) under NSF cooperative agreement  
466 GEO-1240507 and the Penn State Center for Climate Risk Management (CLIMA). All  
467 views, errors, and opinions are solely that of the authors.



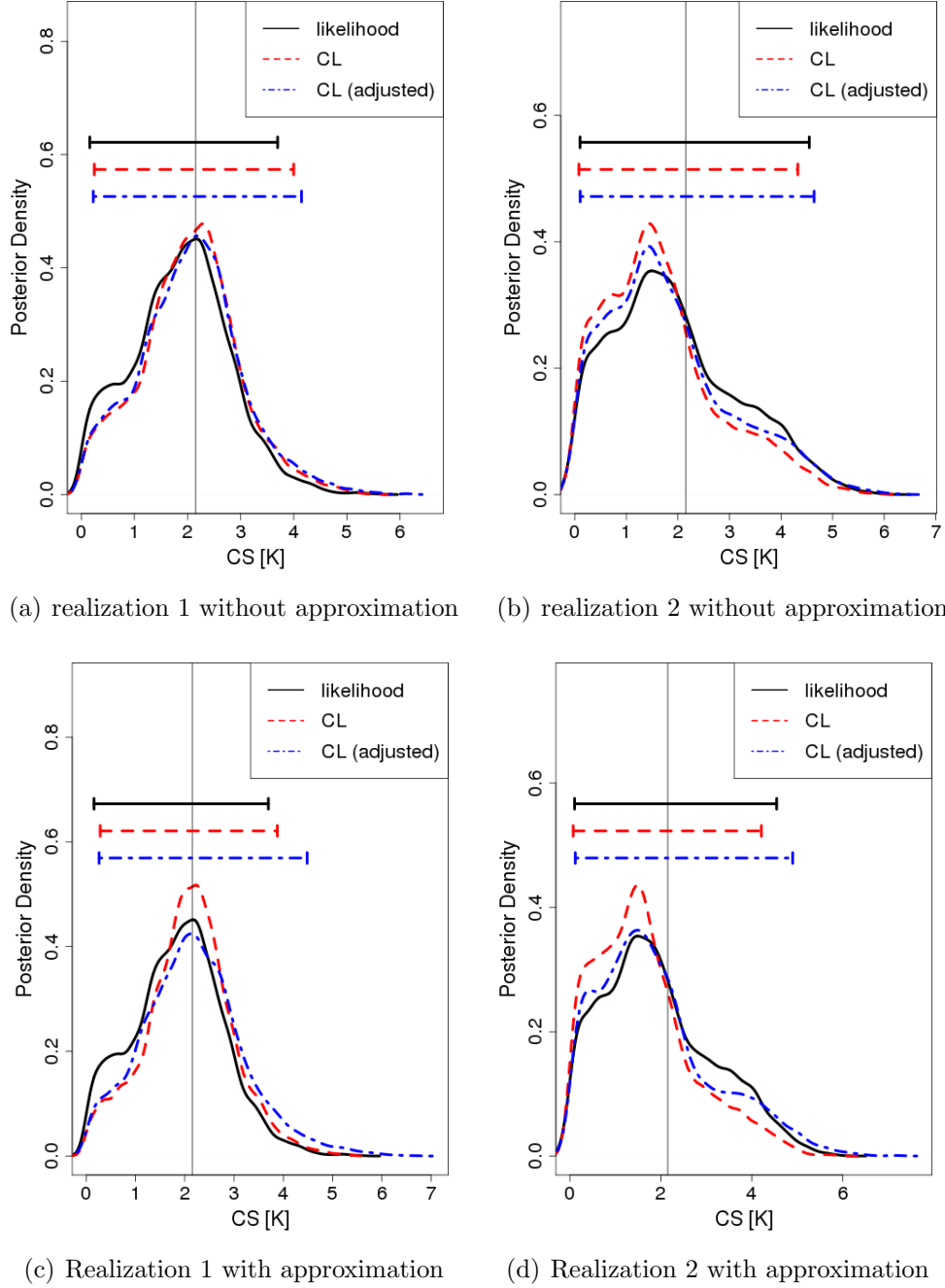


Figure 1: Comparison between calibration results using i) the original likelihood without blocking (solid black curves), ii) the block composite likelihood without the variance adjustment (dashed red line), and iii) the block composite likelihood with the variance adjustment (dashed-dotted blue line). The vertical lines represent the assumed true value for our simulation, and the horizontal bars above show the 95% credible intervals. The results shown here are based on two different realizations (two left panels for Realization 1 and two right panels for Realization 2) from the same GP model. The posterior densities with the approximation for the block means (two lower panels) are reasonably close to the densities without the approximation (two upper panels) when the variance adjustment is applied.

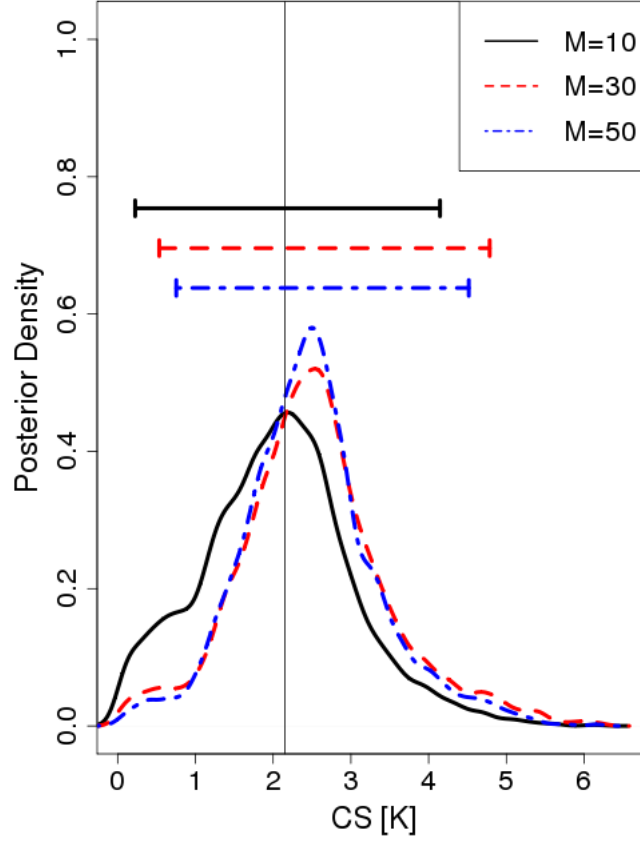


Figure 2: Comparison of posterior densities between three simulated examples with different block numbers:  $M = 10$  (solid black curve),  $M = 30$  (dashed red curve), and  $M = 50$  (dotted-dashed blue curve). The vertical line is the assumed true value for our simulated example and the horizontal bars above are 95% credible intervals. Posterior modes based on 30 and 50 blocks show slight biases, but the width of interval does not show notable differences.

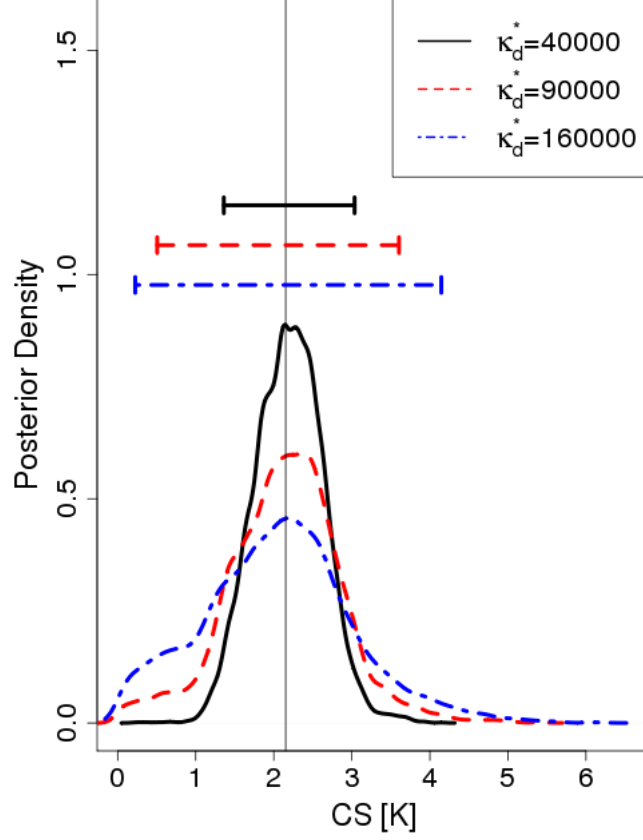


Figure 3: Comparison of posterior densities between three simulated examples with different assumed magnitudes of the discrepancies:  $\kappa_d^* = 40000$  (solid black curve),  $\kappa_d^* = 90000$  (dashed red curve), and  $\kappa_d^* = 160000$  (dotted-dashed blue curve). The vertical line indicates the assumed true values, and the horizontal bars above show the 95% credible intervals. As the discrepancy grows, the densities become more dispersed but the posterior modes stay similar.

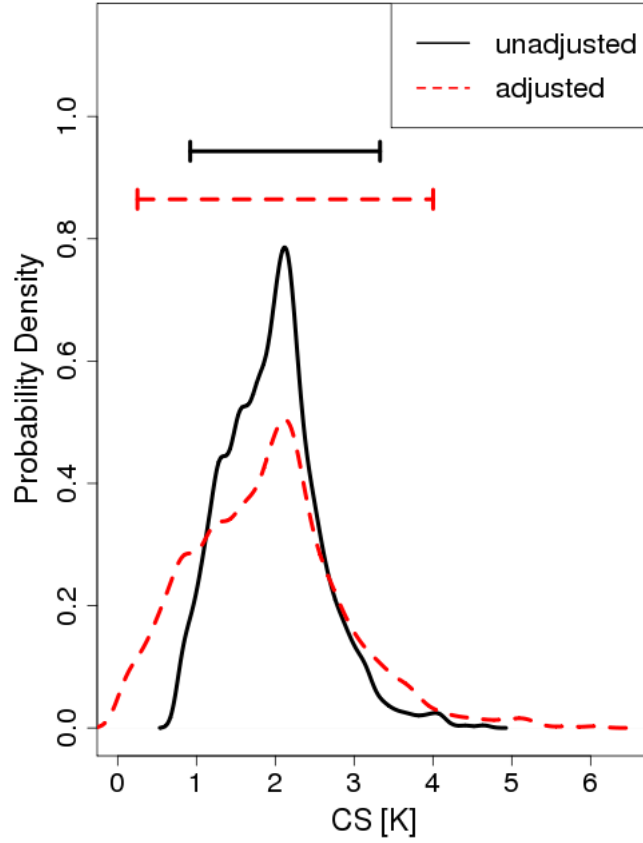


Figure 4: Posterior densities of the climate sensitivity calibrated based on the observational data from Levitus et al. (2012) using our composite likelihood approach. The adjusted posterior density (solid black curve) is notably more dispersed than the unadjusted one (dashed black curve), and the corresponding 95% credible intervals (horizontal bars above) for the adjusted posterior density is also much wider than the one for the unadjusted density.

## References

- Andronova, N., Schlesinger, M., Dessai, S., Hulme, M., and Li, B. (2007), *The concept of climate sensitivity: History and development*, in *Human-induced Climate Change: An Interdisciplinary Assessment*, edited by M. Schlesinger, H. Kheshgi, J. Smith, F. de la Chesnaye, J. M. Reilly, T. Wilson, and C. Kolstad, Cambridge University Press, New York.
- Arendt, P. D., Apley, D. W., and Chen, W. (2012), “Quantification of Model Uncertainty: Calibration, Model Discrepancy, and Identifiability,” *J. Mech. Design*, 134, 100908.
- Bayarri, M., Berger, J., Cafeo, J., Garcia-Donato, G., Liu, F., Palomo, J., Parthasarathy, R., Paulo, R., Sacks, J., and Walsh, D. (2007), “Computer model validation with functional output,” *Ann. Statist.*, 35, 1874–1906.
- Berger, J., De Oliveira, V., and Sansó, B. (2001), “Objective Bayesian analysis of spatially correlated data,” *J. Am. Statist. Assoc.*, 96, 1361–1374.
- Besag, J. (1975), “Statistical analysis of non-lattice data,” *Statistician*, 24, 179–195.
- (1977), “Efficiency of pseudolikelihood estimation for simple Gaussian fields,” *Biometrika*, 64, 616–618.
- Bhat, K., Haran, M., and Goes, M. (2010), “Computer Model Calibration with Multivariate Spatial Output: A Case Study,” *Frontiers of Statistical Decision Making and Bayesian Analysis*, 168–184.
- Bhat, K., Haran, M., Olson, R., and Keller, K. (2012), “Inferring likelihoods and climate system characteristics from climate models and multiple tracers,” *Environmetrics*, 23, 345–362.
- Caragea, P. and Smith, R. (2006), “Approximate likelihoods for spatial processes,” *Preprint*.
- Chang, W., Haran, M., Olson, R., and Keller, K. (2013), “Fast dimension-reduced climate model calibration,” *arXiv preprint arXiv:1303.1382*.

494 Chernozhukov, V. and Hong, H. (2003), “An MCMC approach to classical estimation,”  
495 *J. Econometrics*, 115, 293–346.

496 Cooley, D., Ribatet, M., and Davison, A. (2011), “Bayesian inference from composite  
497 likelihoods, with an application to spatial extremes,” *arXiv preprint arXiv:0911.5357*.

498 Cox, D. and Reid, N. (2004), “A note on pseudolikelihood constructed from marginal  
499 densities,” *Biometrika*, 91, 729–737.

500 Cressie, N. (1993), *Statistics for spatial data*, Wiley, New York.

501 Curriero, F. C. and Lele, S. (1999), “A composite likelihood approach to semivariogram  
502 estimation,” *J. Agric. Biol. Environ. Stat.*, 4, 9–28.

503 Eidsvik, J., Shaby, B., Reich, B., Wheeler, M., and Niemi, J. (2013), “Estimation and  
504 prediction in spatial models with block composite likelihoods,” *J. Comp. Graph. Stat.*,  
505 in press.

506 Flegal, J. M., Haran, M., and Jones, G. L. (2008), “Markov chain Monte Carlo: Can we  
507 trust the third significant figure?” *Stat. Sci.*, 23, 250–260.

508 Godambe, V. (1960), “An optimum property of regular maximum likelihood estimation,”  
509 *Ann. Math. Stat.*, 31, 1208–1211.

510 Hansen, J., Russell, G., Lacis, A., Fung, I., Rind, D., and Stone, P. (1985), “Climate  
511 response times - dependence on climate sensitivity and ocean mixing,” *Science*, 229,  
512 857–859.

513 Heagerty, P. J. and Lele, S. R. (1998), “A composite likelihood approach to binary spatial  
514 data,” *J. Am. Statist. Assoc.*, 93, 1099–1111.

515 Higdon, D., Gattiker, J., Williams, B., and Rightley, M. (2008), “Computer model cali-  
516 bration using high-dimensional output,” *J. Am. Statist. Assoc.*, 103, 570–583.

517 Higdon, D., Reese, C., Moulton, J., Vrugt, J., and Fox, C. (2009), “Posterior exploration  
518 for computationally intensive forward models,” *Handbook of Markov Chain Monte*  
519 *Carlo*.

520 Jones, G., Haran, M., Caffo, B. S., and Neath, R. (2006), “Fixed-width output analysis  
521 for Markov chain Monte Carlo,” *J. Am. Statist. Assoc.*, 101, 1537–1547.

522 Keller, K., Bolker, B., and Bradford, D. F. (2004), “Uncertain climate thresholds and  
523 optimal economic growth,” *J. Environ. Econ. Manage.*, 48, 723–741.

524 Kennedy, M. and O’Hagan, A. (2001), “Bayesian calibration of computer models,” *J. R.*  
525 *Stat. Soc. Ser. B Stat. Methodol.*, 63, 425–464.

526 Knutti, R. and Hegerl, G. C. (2008), “The equilibrium sensitivity of the Earth’s temper-  
527 ature to radiation changes,” *Nat. Geosci.*, 1, 735–743.

528 Knutti, R., Stocker, T. F., Joos, F., and Plattner, G. K. (2002), “Constraints on radiative  
529 forcing and future climate change from observations and climate model ensembles,”  
530 *Nature*, 416, 719–723.

531 Levitus, S., Antonov, J., Boyer, T., Baranova, O., Garcia, H., Locarnini, R., Mishonov,  
532 A., Reagan, J., Seidov, D., Yarosh, E., et al. (2012), “World ocean heat content and  
533 thermosteric sea level change (0–2000 m), 1955–2010,” *Geophys. Res. Lett.*, 39.

534 Lindsay, B. G. (1988), “Composite likelihood methods,” *Contemp. Math.*, 80, 221–39.

535 Mardia, K. V. and Marshall, R. (1984), “Maximum likelihood estimation of models for  
536 residual covariance in spatial regression,” *Biometrika*, 71, 135–146.

537 Nordhaus, W. D. and Boyer, J. (2000), *Warning the World: Economic Models of Global*  
538 *Warming*, MIT Press (MA).

539 Sacks, J., Welch, W., Mitchell, T., and Wynn, H. (1989), “Design and analysis of com-  
540 puter experiments,” *Stat. Sci.*, 4, 409–423.

541 Schmittner, A., Urban, N., Keller, K., and Matthews, D. (2009), “Using tracer observa-  
542 tions to reduce the uncertainty of ocean diapycnal mixing and climate–carbon cycle  
543 projections,” *Global Biogeochem. Cy.*, 23, 737–750.

- 544 Shaby, B. A. (2012), “The open-faced sandwich adjustment for MCMC using estimating  
545 functions,” *arXiv preprint arXiv:1204.3687*.
- 546 Stein, M. L., Chi, Z., and Welty, L. J. (2004), “Approximating likelihoods for large spatial  
547 data sets,” *J. R. Stat. Soc. Ser. B Stat. Methodol.*, 66, 275–296.
- 548 Urban, N. and Keller, K. (2010), “Probabilistic hindcasts and projections of the cou-  
549 pled climate, carbon cycle and Atlantic meridional overturning circulation system: a  
550 Bayesian fusion of century-scale observations with a simple model,” *Tellus A*, 62, 737–  
551 750.
- 552 Varin, C. (2008), “On composite marginal likelihoods,” *Adv. Stat. Anal.*, 92, 1–28.
- 553 Vecchia, A. V. (1988), “Estimation and model identification for continuous spatial pro-  
554 cesses,” *J. R. Stat. Soc. Ser. B Stat. Methodol.*, 50, 297–312.
- 555 Weaver, A., Eby, M., Wiebe, E., Bitz, C., Duffy, P., Ewen, T., Fanning, A., Holland, M.,  
556 MacFadyen, A., and Matthews, H. (2001), “The UVic Earth System Climate Model:  
557 Model description, climatology, and applications to past, present and future climates,”  
558 *Atmos.-Ocean.*, 39, 361–428.
- 559 Wynn, H. (2001), “Contribution to the discussion on the paper by Kennedy and  
560 O’Hagan,” *J. R. Stat. Soc. Ser. B Stat. Methodol.*, 63, 425–464.
- 561 Yakowitz, S. and Szidarovszky, F. (1985), “A comparison of kriging with nonparametric  
562 regression methods,” *J. Multivariate Anal.*, 16, 21–53.
- 563 Zhang, H. and Zimmerman, D. L. (2005), “Towards reconciling two asymptotic frame-  
564 works in spatial statistics,” *Biometrika*, 92, 921–936.